# Analytical and numerical calculation of surface temperature and thermal constriction resistance in transient dynamic strip contact

Nadia Aderghal, Tahar Loulou, Ali Bouchoucha, Philippe Rogeon

# Accepted Manuscript

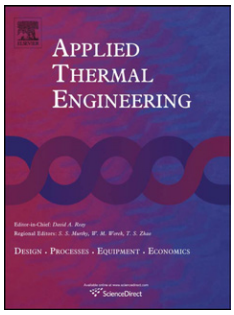


Title: Analytical and numerical calculation of surface temperature and thermal constriction resistance in transient dynamic strip contact

Authors: Nadia Aderghal, Tahar Loulou, Ali Bouchoucha, Philippe Rogeon

PII: S1359-4311(11)00068-8

DOI: 10.1016/j.applthermaleng.2011.01.044

Reference: ATE 3408

To appear in: *Applied Thermal Engineering*

Received Date: 9 July 2010

Revised Date: 19 January 2011

Accepted Date: 27 January 2011

Please cite this article as: N. Aderghal, T. Loulou, A. Bouchoucha, P. Rogeon. Analytical and numerical calculation of surface temperature and thermal constriction resistance in transient dynamic strip contact, Applied Thermal Engineering (2011), doi: 10.1016/j.applthermaleng.2011.01.044

# Analytical and numerical calculation of surface temperature and thermal constriction resistance in transient dynamic strip contact

Nadia Aderghal[1,2,3], Tahar Loulou[1,*], Ali Bouchoucha[2] and Philippe Rogeon[1]

[1] Université de Bretagne Sud, Centre de Recherche, LIMATB
F-56321, Lorient, France

[2] Faculté des Sciences de l'Ingénieur, Laboratoire de Mécanique,
Campus Chaabat-Erssas, Université Mentouri, Constantine, 25000, Algeria

[3] Département de Génie Mécanique,
Université de Jijel, BP 98, Ouled Aissa, Jijel, 18000, Algeria

tahar.loulou@univ-ubs.fr

January 19, 2011

**Abstract**

In this paper, the problem of transient heat transfer in sliding contact is studied analytically and numerically. The heat source is represented as a uniform heat strip moving over a half-space with and without cooling outside the contact zone. The finite element method, implemented using a commercial code, was used in numerically solving this problem. An analytical solution taken from the literature was adapted to obtain the presented model and used to check the capabilities of the commercial code. After the validation of the resolution method, the work was completed by studying the influence of the Peclet number (source speed) and the Biot number (presence of cooling) on the temporal and spatial evolution of the surface temperature of the half-space. Finally, the transient constriction function is estimated and analyzed for the presented test cases. Correlations were also derived to (i) evaluate the time interval within which the steady state is reached, and (ii) estimate the constriction parameter as a function of Peclet and Biot numbers in the steady state case.

**Keywords:** dimensionless constriction, thermal resistance, heat flux channel, surface temperature, moving strip heat source.

*Corresponding author

## Nomenclature

| | | |
|---|---|---|
| $a$ | half strip width | m |
| $A_c$ | contact area | $m^2$ |
| $A_0$ | half space surface | $m^2$ |
| $b$ | half medium width | m |
| $Bi$ | Biot number | |
| $c$ | strip length | m |
| $Fo$ | Fourier number | |
| $h$ | heat convection coefficient | $W/m^2K$ |
| $k$ | thermal conductivity | W/mK |
| $L$ | reference length | m |
| $Pe$ | Peclet number | |
| $q$ | applied heat flux | $W/m^2$ |
| $Q(t)$ | heat flow rate | W |
| $R_c(t)$ | constriction resistance | k/W |
| $T(x,z,t)$ | temperature field | K |
| $\bar{T}_0(t)$, $\bar{T}_c(t)$ | average temperature | K |
| $t$, $t'$ | time | s |
| $V$ | sliding speed | m/s |
| $x$, $z$ | space coordinates | m |

## Greek symbols

| | | |
|---|---|---|
| $\alpha$ | thermal diffusivity | $m^2/s$ |
| $\epsilon$ | constriction ratio | |
| $\psi$ | dimensionless constriction resistance | |

## Subscript

| | |
|---|---|
| $c$ | contact |
| $i$ | initial |
| $r$ | reference |
| $ss$ | steady state |
| $\infty$ | far from the contact |

## Superscript

| | |
|---|---|
| $+$ | dimensionless variable |

## Introduction

Generated heat at the surface of one body or at the contact interface between two bodies in industrial processes, such as laser welding, braking systems, friction between two mediums and so on, is often modeled by using the concept of moving heat source in stationary or transient case. Most of this heat is expended on the increases in the temperature of the contact interface. This local temperature increase can strongly affect the surface properties of materials. Thus, the temperature level plays an important role in various applications and should be carefully controlled.

Although this is a very old subject, it remains scientifically important and at the microscopic scale, difficult to master in some configurations, such as transitional arrangements and the presence of heat convection. The study of heating due to friction has been the subject of many research works during the last century. Indeed, several publications have reported attempts at finding the transient temperature rise or the heat transfer rate within a circular disk (contact area) which is moving on the surface of an isotropic half-space. These solutions are presented for (i) the transient heat flow rate from the contact area when the contact area is isothermal, and (ii) the temperature rise of the contact area when the area is subjected to any heat flux profile. Several studies based on the moving heat source theory have been developed in order to calculate the average temperature over the contact area [1–7].

The previous investigations can be divided into two categories: (i) analytical solutions which are possible in some special cases of geometry and boundary conditions giving unlimited information over the entire range of dimensionless time [2, 4, 8–14], and (ii) numerical methods that provide results for practically any combination of geometry and boundary conditions, but the results of which must be presented as a correlation to be useful [15–19].

Most authors have thoroughly investigated the case of a semi-infinite solid heated by a spot or strip moving source and insulated outside the contact zone [1–5, 7–11]. A few studies have been conducted on the problem presented here, but they used cooling at the surface of the half-space [16, 20–26]. All these studies consisted of calculating the temperature in a semi-infinite body subjected to a spot or a strip of heat flux on its surface and where the fundamental reference of Jaeger et al. [1, 2] is the starting point in all of the theoretical developments. Up to now, some practical and very interesting problems remain unresolved. For most of them, analytical methods are unpracticable and the use of numerical tools is the only way to solve these important cases.

The work proposed in this paper aims at analytically and numerically predicting the evolution of the temperature and thermal constriction resistance of a semi-infinite body subjected to a moving band heat source in transient and steady state with and without heat convection outside the contact area. Knowledge of these quantities is essential to define the partition of the heat flux generated at the interface by the friction between two sliding solids.

The paper contains four sections, including the present introduction. Section two presents the statement of the problem with a physical dimension and, for generality, also in a dimensionless form. In section three, analytical solutions (in transient and steady state cases) for the temperature distribution in this particular case are developed from the classical solution established by Jaeger and Carslaw [1]. To complete this investigation, numerical solutions are developed (finite element method) to determine the temperature distribution with and without convection outside the contact area. The numerical values will be presented in tables, and when possible, correlation equations will be given. The provided solutions can be used for static and sliding contact cases, as well as for the analysis of the presence of cooling on the temperature distribution.

## Problem formulation

Consider a strip heat source of width $2a$ moving along the surface of a semi-infinite body initially at a uniform temperature $T_i$. This source is moving opposite of x-direction with a constant speed, see figure (1). The moving source generates a transient temperature field in the semi-infinite medium described by the following model:

$$\frac{\partial^2 T}{\partial x^2} + \frac{\partial^2 T}{\partial z^2} - \frac{V}{\alpha}\frac{\partial T}{\partial x} = \frac{1}{\alpha}\frac{\partial T}{\partial t} \tag{1}$$

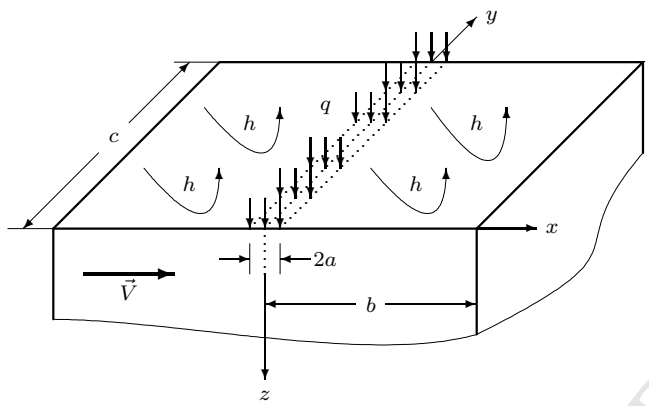


Figure 1: Geometric configuration and coordinate system.

$$-k\frac{\partial T}{\partial z} = \begin{cases} q & -a \le x \le +a \\ h\left[T_\infty - T\right] & x < -a \quad \text{and} \quad x > +a \end{cases} \qquad z = 0 \tag{2}$$

$$\left.\frac{\partial T}{\partial x}\right|_{x=-b} = \left.\frac{\partial T}{\partial x}\right|_{x=+b} = 0 \qquad \text{for} \qquad 0 < z < \infty \tag{3}$$

$$T(x,z,t) = T_i \qquad \text{when} \qquad z \longrightarrow \infty \tag{4}$$

$$T(x,z,t) = T_i \quad \text{to} \quad t = 0 \tag{5}$$

The initial temperature $T_i$ and the ambient temperature $T_\infty$ are both assumed constant and equal to zero.

In the present problem, heat enters the half-space, supposed to be isotropic, over the contact area (strip). The constriction resistance arises due to the fact that the contact width is smaller than the width of the semi-infinite solid which results in forcing the heat flow lines to spread out into the semi-infinite solid. As the source is infinite in the y-direction, the temperature field in the half-space is two dimensional, transient, and termed $T(x,z,t)$. In order to calculate the transient thermal constriction resistance $R_c(t)$, we use the following definition given by Carslaw [1], Yovanovich [27,28], Negus [29], and Madhusudana [30]:

$$R_c(t) = \frac{\bar{T}_c(t) - \bar{T}_0(t)}{Q(t)} \tag{6}$$

where $\bar{T}_c(t)$ is the average temperature over the contact area $A_c = 2a$ and $\bar{T}_0(t)$ is the average temperature over the infinite contact plan $z = 0$ named $A_0$ in this case. The infinite length of the y-direction requires the use of one length unit in this direction for computation. Mathematically speaking, both of these temperatures are computed by the following two integrals:

$$\bar{T}_c(t) = \frac{1}{A_c}\int_{-a}^{+a} T(x,0,t)\,dx \qquad \text{and} \qquad \bar{T}_0(t) = \frac{1}{A_0}\int_{-\infty}^{+\infty} T(x,0,t)\,dx \tag{7}$$

Quantity $Q(t)$ is the total heat flow rate across the contact area ($Q = qA_c$). In the half space configuration, the average temperature $\bar{T}_0(t)$ is assumed to be zero (equal to the initial temperature).

For the sake of generality, we introduce the following dimensionless variables:

$$x^+ = \frac{x}{L} \qquad z^+ = \frac{z}{L} \qquad a^+ = \frac{a}{L} \qquad b^+ = \frac{b}{L} \qquad t^+ = \frac{\alpha t}{L^2}, \qquad t'^+ = \frac{\alpha t'}{L^2} \qquad T^+ = \frac{T - T_i}{T_r} \tag{8}$$

$$Fo = \frac{\alpha(t - t')}{L^2}, \qquad Pe = \frac{VL}{\alpha}, \qquad Bi = \frac{hL}{k}, \qquad \epsilon = \frac{a}{b}, \qquad T_r = \frac{qL}{k} \qquad Q_r = qL \tag{9}$$

where $L$ is the reference length, which can be $a$, $2a$, $a/2$ or any other suitable reference length. The above system of equations in dimensionless form becomes (signs + are omitted for better presentation):

$$\frac{\partial^2 T}{\partial x^2} + \frac{\partial^2 T}{\partial z^2} - Pe\frac{\partial T}{\partial x} = \frac{\partial T}{\partial t} \tag{10}$$

$$-\frac{\partial T}{\partial z} = \begin{cases} 1 & -1 \le x \le +1 \\ -Bi\,T & x < -1 \quad \text{and} \quad x > +1 \end{cases} \qquad z = 0 \tag{11}$$

$$\left.\frac{\partial T}{\partial x}\right|_{x=-1/\epsilon} = \left.\frac{\partial T}{\partial x}\right|_{x=+1/\epsilon} = 0 \qquad \text{for} \qquad 0 < z < \infty \tag{12}$$

$$T(x,z,t) = 0 \qquad \text{when} \qquad z \longrightarrow \infty \tag{13}$$

$$T(x,z,t) = 0 \quad \text{at} \quad t = 0 \tag{14}$$

where constants $Pe$ and $Bi$ represent the Peclet and Biot numbers, respectively, and $\epsilon$ the constriction parameter.

For the dimensionless transient spreading resistance of an isoflux (*uniform heat flux distribution over the strip*) strip of width $2a$ within a two-dimensional channel of width $2b$, unit length, constant thermal properties were reported as [27, 31–33]:

$$\psi(t) = kR_c(t) \tag{15}$$

The constriction resistance depends on the heat flux distribution over the source area and the shape and aspect ratio of the contact area.

**Choice of mesh:** To validate our numerical results with the available analytical solution given in the literature for some special cases and to get as close as possible to the semi-infinite configuration, we have taken a constriction ratio (or constriction parameter) $\epsilon = a/b = 0.0001$. The accurate determination of temperature distribution and constriction resistance for the study of moving contacts, and particularly for small values of epsilon, requires meticulous attention to the choice of the space mesh. For these purposes, a study consisting of choosing the appropriate mesh was undertaken. To best follow the spatial evolution of temperature fields, in the vicinity of the contact zone, we chose a very small mesh along the path of the heat source and gradually increased it away from the contact area. Similarly for the dimension time, a very small step was adopted to reduce and limit the numerical instabilities associated with this numerical resolution. The choice of the space and time steps is very important for the accuracy of the numerical results of this type of problem. The present study uses the finite element package COMSOL MULTIPHYSICS SOFTWARE® [34] with the following technical details: (i) number of nodes 4467 (ii) number of elements 21485, (iii) minimum element quality 0.696, (iv) triangular element, (v) Lagrange quadratic element, (vi) GMRES solver, and (vii) logarithmic time increment starting from $t_{min} = 10^{-5}$ to $t_{max} = 10^4$ with 910 time steps.

## Results and discussion

The temperature field from the passage of the moving heat source is studied in the linear case where the constituent material is assumed isotropic, uniform, and has constant thermophysical parameters. In the first part of this work, the problem is solved in the case of adiabatic conditions, i.e. without cooling outside the contact area. For this special case, $Bi = 0$, an analytical solution exists in the literature [1, 2] , but it is presented in a different dimensionless form which makes the comparison slightly difficult to conduct and to understand. The required analytical developments and transformations conducted on the existing analytical solution are summarized in what follows.

The starting point is the classical rectangular source solution, given in Jaeger [2], equation (19) page 209, and reported here:

$$T(x,y,z,t) = \frac{\alpha q}{4k(\alpha\pi)^{3/2}} \int_0^t \frac{dt'}{(t-t')^{3/2}} \int_{-a}^{+a} \left[ \int_{-c}^{+c} \exp\left[ -\frac{\left[x - x' - V(t-t')\right]^2 + (y-y')^2 + z^2}{4\alpha(t-t')} \right] dy' \right] dx' \tag{16}$$

It represents the solution of a rectangular source with sides $2a$ parallel to the $x$-axis and $2c$ parallel to the $y$-axis at time $t$. This source is moving with a finite velocity $V$ along the x-axis in the plane $z = 0$ with no heat losses outside

the contact area. By introducing the dimensionless quantities given in equations (8) and (9) into the above equation (16), and defining $C = c/L$ as the dimensionless distance along the $y$-axis, we obtain the following dimensionless solution for the moving rectangular heat source:

$$\begin{aligned} T(x,y,z,t) &= \frac{1}{4\sqrt{\pi}}\int_0^t \exp\Big[-\frac{z^2}{4Fo}\Big] \\ &\times \Big[\mathrm{erf}\Big[\frac{x+a-PeFo}{2\sqrt{Fo}}\Big] - \mathrm{erf}\Big[\frac{x-a-PeFo}{2\sqrt{Fo}}\Big]\Big] \\ &\times \Big[\mathrm{erf}\Big[\frac{C+y}{2\sqrt{Fo}}\Big] + \mathrm{erf}\Big[\frac{C-y}{2\sqrt{Fo}}\Big]\Big]\frac{dFo}{\sqrt{Fo}} \end{aligned} \tag{17}$$

This solution is given in Laraqi [9]. The analytical solution of our two-dimensional geometric configuration is immediately obtained by letting $C \longrightarrow \infty$ which gives:

$$T(x,z,t) = \frac{1}{2\sqrt{\pi}}\int_0^t \exp\Big[-\frac{z^2}{4Fo}\Big]\Big[\mathrm{erf}\Big[\frac{x+a-PeFo}{2\sqrt{Fo}}\Big] - \mathrm{erf}\Big[\frac{x-a-PeFo}{2\sqrt{Fo}}\Big]\Big]\frac{dFo}{\sqrt{Fo}} \tag{18}$$

The surface temperature of the semi-infinite medium is obtained by putting $z = 0$ in the previous equation which reduces to:

$$T(x,0,t) = \frac{1}{2\sqrt{\pi}}\int_0^t \Big[\mathrm{erf}\Big[\frac{x+a-PeFo}{2\sqrt{Fo}}\Big] - \mathrm{erf}\Big[\frac{x-a-PeFo}{2\sqrt{Fo}}\Big]\Big]\frac{dFo}{\sqrt{Fo}} \tag{19}$$

The average contact temperature is obtained analytically by the following integration:

$$\begin{aligned} \bar{T}_c(t) &= \frac{1}{2a}\int_{-a}^{+a} T(x,0,t)dx \\ &= \frac{1}{2a\sqrt{\pi}}\int_0^t \Big[\phi(u) + \phi(v) - 2\phi(w)\Big]dFo \end{aligned} \tag{20}$$

where the function $\phi$ is defined by:

$$\phi(s) = s\,\mathrm{erf}(s) + \frac{1}{\sqrt{\pi}}\exp\big[-s^2\big] \tag{21}$$

and the dummy variables $u$, $v$, and $w$ are given by:

$$u = \frac{-PeFo + 2a}{2\sqrt{Fo}} \qquad v = \frac{-PeFo - 2a}{2\sqrt{Fo}} \quad \text{and} \quad w = \frac{-PeFo}{2\sqrt{Fo}}$$

Surface temperature T(x,0,t) and average temperature $\bar{T}_c(t)$, given respectively in equations (19) and (20), are more general than those given in reference [2] in the sense that they give the temperature level over the contact zone and the plane $z = 0$ in both cases: static $Pe = 0$ and dynamic $Pe \neq 0$ for transient and steady states.

**Static heat source:** In the static contact case, the source is stationary which corresponds to Peclet number $Pe = 0$. In this case, the analytical integration of equations (19) and (20) gives the following expressions:

$$T(x,0,t) = \sqrt{\frac{t}{\pi}}\Big[\mathrm{erf}\Big(\frac{a+x}{\sqrt{4t}}\Big) + \mathrm{erf}\Big(\frac{a-x}{\sqrt{4t}}\Big) - \Big(\frac{a+x}{\sqrt{4\pi t}}\Big)\mathrm{Ei}\Big(-\frac{(a+x)^2}{4t}\Big) - \Big(\frac{a-x}{\sqrt{4\pi t}}\Big)\mathrm{Ei}\Big(-\frac{(a-x)^2}{4t}\Big)\Big] \tag{22}$$

$$\bar{T}_c(t) = \frac{1}{2a\sqrt{\pi}}\Big[2\sqrt{t}\,\mathrm{erf}\Big(\frac{a}{\sqrt{t}}\Big) + \frac{t}{\sqrt{\pi}}\Big(\exp\Big[-\frac{a}{t}\Big] - 1\Big) + \frac{a}{\sqrt{\pi}}\mathrm{Ei}\Big(-\frac{a}{t}\Big) - \frac{2a}{\sqrt{\pi}}\mathrm{Ei}\Big(-\frac{a^2}{t}\Big)\Big] \tag{23}$$

In our case, the characteristic length was taken as $L = a$, i.e. the half width of the heating source which significantly reduces the above equations. From its definition given in equation (15), the dimensionless thermal constriction resistance is computed by:

$$\psi(t) = \frac{\bar{T}_c(t)}{2} \tag{24}$$

This analytical solution will first be used to test the capabilities of the finite element method in handling this problem.

| $t$ | $10^{-4}$ | $10^{-3}$ | $10^{-2}$ | $10^{-1}$ | $10^{+0}$ | $10^{+1}$ | $10^{+2}$ | $10^{+3}$ | $10^{+4}$ |
|---|---|---|---|---|---|---|---|---|---|
| Numerically | 0.005 | 0.017 | 0.054 | 0.160 | 0.406 | 0.751 | 1.115 | 1.483 | 1.846 |
| Analytically | 0.005 | 0.017 | 0.054 | 0.162 | 0.409 | 0.754 | 1.118 | 1.485 | 1.851 |

Table 1: Comparison of constriction resistance between analytical and numerical solutions. These values are displayed graphically in Figure (2).

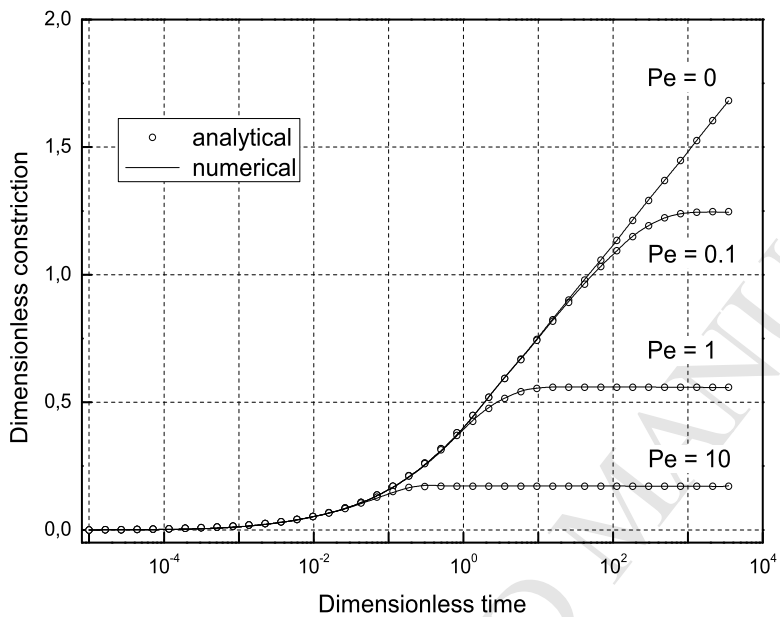


Figure 2: Transient constriction resistance in semi-infinite strip for different Peclet numbers.

Figure (2) shows the evolution of the dimensionless thermal constriction resistance as a function of the dimensionless time computed analytically by equation (24) and obtained numerically by the finite element method when $Pe = 0$. The comparison of these results shows good correlation between the two solutions. As is well-known, the transient resistance in the static case ($Pe = 0$) does not reach the steady state [27]. Some of the numerical values of both results are displayed in Table (1). The presented numerical values correspond well with the analytical ones and the numerical estimation of the thermal constriction resistance is easily obtained.

**Moving heat source**: In a second stage, the finite element method is used to solve the problem when the heat source is not stationary i.e. $Pe \neq 0$ without cooling at the surface. Figure (2) displays both numerical and analytical solutions for some of the values of Peclet number $Pe$. The analytical solution is obtained successively from equations (20) and (24), while the second one is computed by the finite element code. Figure (2) shows the results of three tests: $Pe = 0.1$, $Pe = 1$, and $Pe = 10$.

As displayed by Figure (2), the numerical solution precisely matches the analytical one over the whole time domain. As the Peclet number increases, the steady state constriction resistance decreases and the steady state is quickly reached. When the Peclet number changes from 0.1 to 10, i.e. the speed of the heat source is increased 100 times, the constriction resistance reduces from 1.246 to 0.170 which is approximately 7 times less. From the analysis of the steady state behavior of the constriction resistance, the time for which the steady state is reached is computed and can be roughly estimated by the following formula:

$$t_{ss} = 69.14 Pe^{-1.91} \tag{25}$$

for a Peclet number in the range $0.1 \leq Pe \leq 20$. This steady state time $t_{ss}$ was established by analyzing the asymp-

totic behavior of the constriction resistance and using a nonlinear least square fit. In other words, when the variation between two successive values of this resistance is less than 0.1 % the steady state is supposed to be achieved. This formula has the advantage of giving the limit time for which the thermal constriction is established, as well as the kind of simplifying assumptions that can be applied.

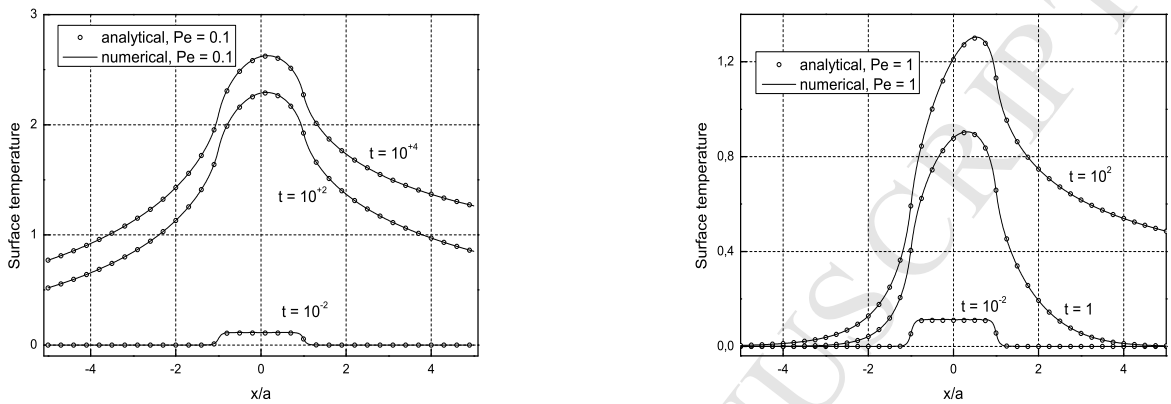


Figure 3: Evolution of surface temperature as a function of time and for different Peclet number values.

Figure (3) displays the surface temperature of the semi-infinite medium, over and outside the contact zone, for two values of the Peclet number at three specific time steps. The last and greatest time step corresponds to the establishment of the steady state regime for both Peclet numbers. For $Pe = 0.1$, there is no substantial change in the space distribution of the surface temperature of the half-space when the time is equal to or greater than $10^4$. To make the paper self contained, the analytical solution of the steady state, according to the previous dimensionless variables, is given below:

$$T(x,z) = \frac{1}{\pi}\int_{-a}^{+a} \exp\left(\frac{Pe}{2}(x-s)\right) \mathrm{K}_0\left(\frac{Pe}{2}\sqrt{(x-s)^2+z^2}\right) ds \tag{26}$$

where $\mathrm{K}_0(x)$ is the modified Bessel function of the second kind of order zero. As expected and as can be observed in Figure (3), the highest temperature occurs in the contact zone $-1 < x/a < +1$. The maximum temperature in the contact area decreases when the Peclet number increases. In other words, when the speed of the heat source increases, the heat has less time to diffuse in the half-space.

The temperature distribution along the sliding direction passing through the center of the heat source at different Peclet numbers is shown in Figure (4). Indeed, in the immediate passage of the source, the heat flux received by the solid is redistributed by diffusion and transport in the half-space. This figure shows that the peak of the maximum temperature reached on the contact zone moves towards the boundary of the latter with the increase in the Peclet number. This result is well known in the literature [1]. By observing the curves of the temperature distribution, it can be noted that the surface temperature in the contact area ($-a < x < +a$) is significantly affected by the heat flux distribution. While the shape of the heat flux distribution has little effect on the temperature distribution outside the area of the heat source. For low velocities, the temperature is distributed almost symmetrically with a maximum in the vicinity of the center of contact. As the sliding velocity increases, the maximum shifts in the direction opposite of the sliding direction, and it occurs at the outlet from contact at high velocities.

Figure (5) represents the spatial distribution of temperature in the semi-infinite solid as a function of $x/a$ for different values of $Pe$ and depth $z$. The most important variations for the temperature arise in the plane of the source $z = 0$. The maxima of the curves are seen to move steadily to the right as $z$ increases. This effect is caused by diffusion and transport of heat from the contact surface inwards after the source has passed.

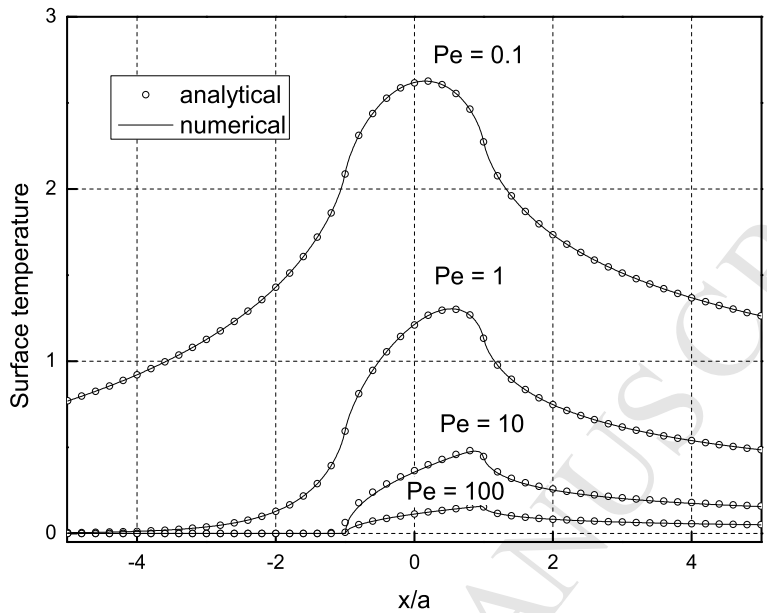


Figure 4: Surface steady state temperature as a function of Peclet number.

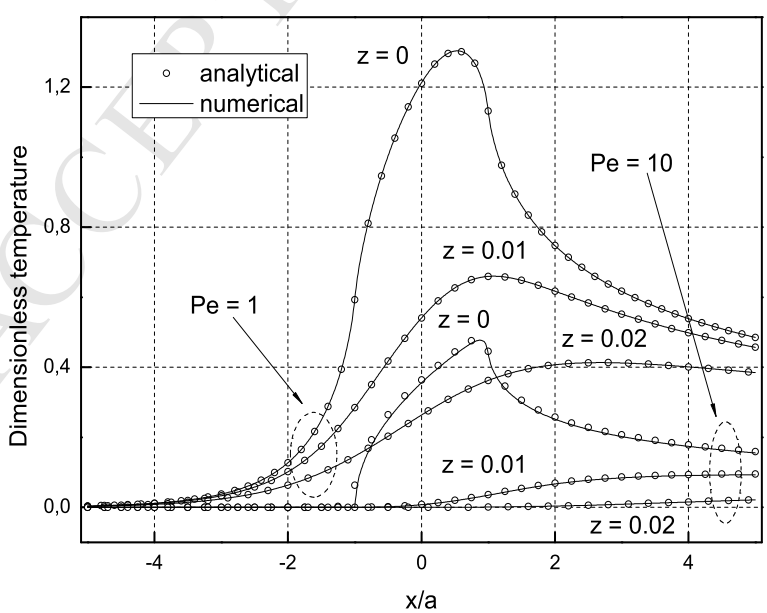


Figure 5: Steady state temperature as a function of depth and Peclet number

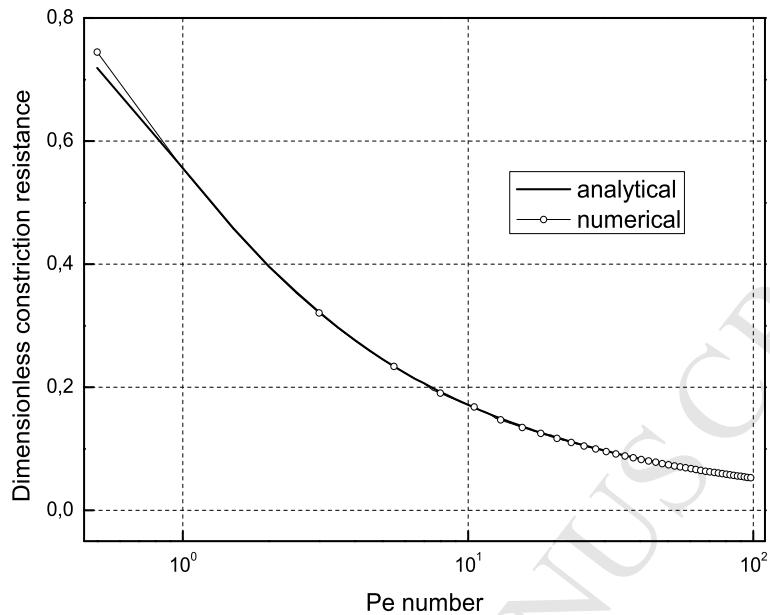


Figure 6: Steady state constriction resistance as a function of Peclet number

In all the previous figures (2)-(5), both analytical and numerical results are displayed simultaneously. This comparison can be done because analytical solutions are available in the literature when the source is moving over an adiabatic surface (no heat convection outside the contact area). The numerical results correlate very well with the analytical ones and the error between them is less than 0.1 % for all of the presented test cases. As a conclusion, the finite element method gives practically the same results and can therefore be used to analyse cases in which the analytical tool proves very difficult to manipulate or are even impracticable.

To determine the steady state constriction resistance, in the case of a moving heat source, we use equations (20) and (24) for time $t$ going to infinity. Figure (6) shows the evolution of steady state constriction $\psi_{ss}$ as a function of the Peclet number. By examining this figure, one can observe that the value of $\psi_{ss}$ cannot be evaluated at $Pe = 0$ when $t \longrightarrow \infty$ (no limit for equation (20) in this case).

The constriction resistance at $Pe = 0.5$ is approximately $\psi_{ss} = 0.718$. From Figure (6), the constriction resistance decreases very quickly in the Peclet number range $0 < Pe \leq 25$. In fact, when the Peclet number increases from 0.5 to 25, $\psi_{ss}$ decreases from 0.718 to 0.107 which is approximately a drop of 87.5 %. From $Pe \approx 25$ to 100, the constriction resistance continues to decrease, but very slowly to reach the final value 0.053. In the absence of convection, an analytical solution does exist that can be used to verify the numerical solution. Indeed, Figure (6) shows both analytical and numerical steady state constriction resistance. Except for the small values of the Peclet number ($Pe \leq 0.8$ ), the numerical results precisely match the analytical ones and the error between them is less than 0.5 %.

**Constriction with cooling:** The cooling at the surface of the half-space is expressed with the Biot number. The meaning of the Biot number mentioned here lies slightly outside its theoretical definition in the sense that it does not represent the ratio of the internal resistance to the resistance of the external film resistance. This paper deals with a semi-infinite medium, thus making the choice of the characteristic length within z-direction difficult. In the definition of Biot number, given in equation (9), the characteristic length was taken as $L = a$, where $a$ is the half width of the moving strip.

Analytical solutions for transient and steady state cases are very difficult to obtain for this case which explains the

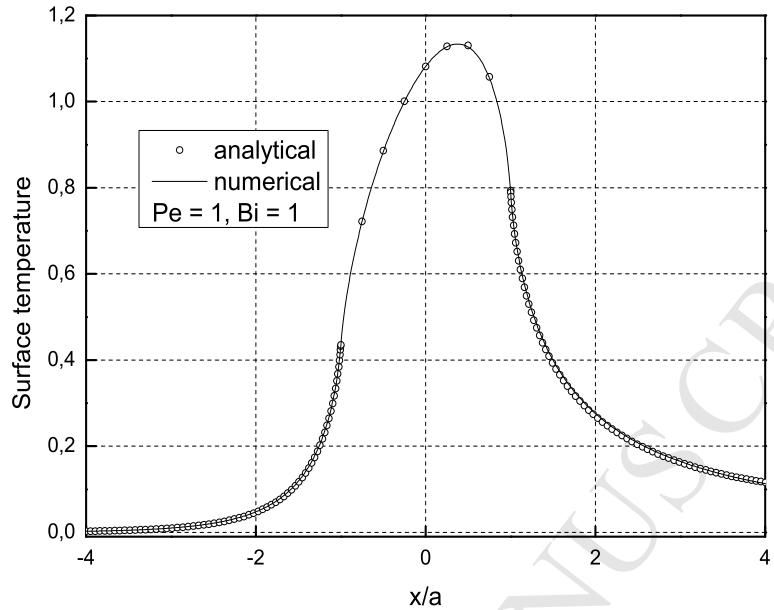


Figure 7: Validation of the finite element method in the case of cooling at the surface.

small number of available analytical solutions in the literature [20, 21]. In the steady state case, Ref. [35] presents the following analytical solution for the surface temperature of semi-infinite medium ($z = 0$), corresponding to the configuration of this paper

$$T(x) = -Bi\int_{-\infty}^{-a} T(s)K(x,s)ds + \int_{-a}^{a} K(x,s)ds - Bi\int_{a}^{\infty} T(s)K(x,s)ds \tag{27}$$

where the kernel $K(x,s)$ is given

$$K(x,s) = \frac{1}{\pi}\exp\left(\frac{Pe}{2}(x-s)\right)\mathrm{K}_0\left(\frac{Pe}{2}|x-s|\right) \tag{28}$$

As one can observe, this solution is presented in the form of an integral equation and the use of numerical integration is the only way to obtain the surface temperature profile. The temperature profile $T(x)$ can easily be obtained from the above equation by application of a gaussian quadrature integration and then the LU decomposition algorithm [36]. This analytical solution is used in this paper to check the solution obtained by the finite element code. Figure (7) displays both analytical and numerical solution for $Pe = 1$ and $Bi = 1$. The error between these two solutions is less than 1 % which confirms the capabilities of the numerical code in solving this problem.

Figure (8) represents the evolution of the dimensionless constriction resistance as a function of time for different values of the Peclet and Biot numbers. The main conclusion of this figure is the decrease of the constriction resistance with the growth of the Peclet and Biot numbers (speed and cooling effect). Specifically, at a low Peclet number ($Pe < 5$), the presence of cooling is significant and affects the surface temperature. At a high Peclet number ($Pe > 10$), the effect of cooling becomes insignificant and can then be neglected.

Figure (9) shows the distribution of temperature at the surface of the half-space with cooling for some time steps and two Peclet numbers, $Pe = 0.1$ and $Pe = 10$. It is interesting in this case to compare the temperature profiles to study the influence of cooling on heat transfer at the surface of the solid. For a low speed, $Pe \leq 0.5$, the surface temperature, outside the contact area, decreases sharply by increasing the convection coefficient which shows the effect of cooling. On the other hand, for higher velocities $Pe \geq 10$, cooling does not present any significant influence on the surface temperature variation. In Figure (9), the maximal surface temperature is observed in the case of an adiabatic surface (no cooling) for all considered time steps and Peclet numbers.

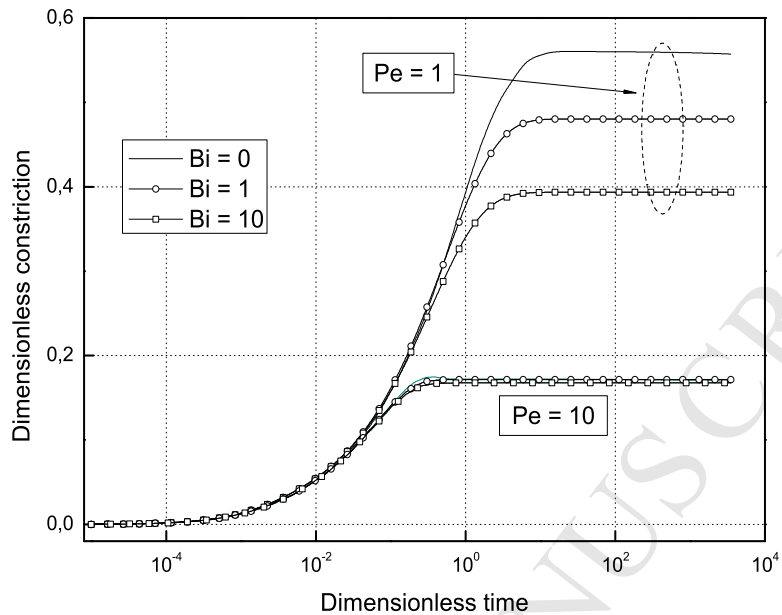


Figure 8: Variation of constriction resistance as a function of time, Peclet number, and cooling (Biot number).

By inspecting the time for which the steady state is established, we see that the surface temperature becomes stationary in less time for high speed generating which is known as "thermal skin". The thermal skin effect becomes more significant with the increase of the source speed and, as a consequence, the heat does not have enough time to diffuse inside the solid. The temperature gradient is confined within a very thin layer in the vicinity of the moving source. The transport term and thermal gradient are of such importance that they require a very fine mesh in and around the contact area. Figure (9) shows the usual curvature of the temperature profile due to the moving heat source, and that the maximum temperature moves to the exit of the contact area when the value of the Peclet number increases.

Figure (10) represents the surface steady state temperature ($z = 0$) for four Peclet numbers (0.1, 1, 10, and 100). In each subfigure, results are shown for different values of Biot 0, 1, and 10. For small Peclet numbers (0.1 and 1), the entire computation region is significantly affected by the convection and the surface temperature distribution is substantially reduced. When the source is moving with high speed (a large Peclet number), the effect of convection varies according to location: before, in, and after the contact zone. The convection has little effect on the temperature at points inside the surface-heating region $-a < x < +a$, but significantly reduces the temperature at all other points.

Figure (11) shows the steady state constriction resistance as a function of Peclet number $Pe$ and for different values of $Bi$ representing the effect of cooling at the interface. All presented curves show a decrease tendency and the highest point is observed with $Bi = 0$ and a very small value of Peclet ($Pe = 0.1$). On the other hand, all the displayed curves come together at a high Peclet number ($Pe \geq 5$). At a low Peclet number, the change of $Bi$ from 0 to 0.5 causes a drop of 44 % of the steady state constriction resistance. At a very high Peclet number ($Pe \approx 100$), there is no difference between the steady state constriction resistances regardless of the value of $Bi$. This means that the cooling becomes insignificant at a high moving speed.

The influence of cooling ($Bi$) on the steady state constriction resistance, for different values of the source speed, is displayed in Figure (12). Except for the window $Bi \times Pe \approx [0, 4] \times [0.1\ 3]$ in which an appreciable change in the steady state constriction resistance can be observed, the above figure shows that the cooling effect is very limited

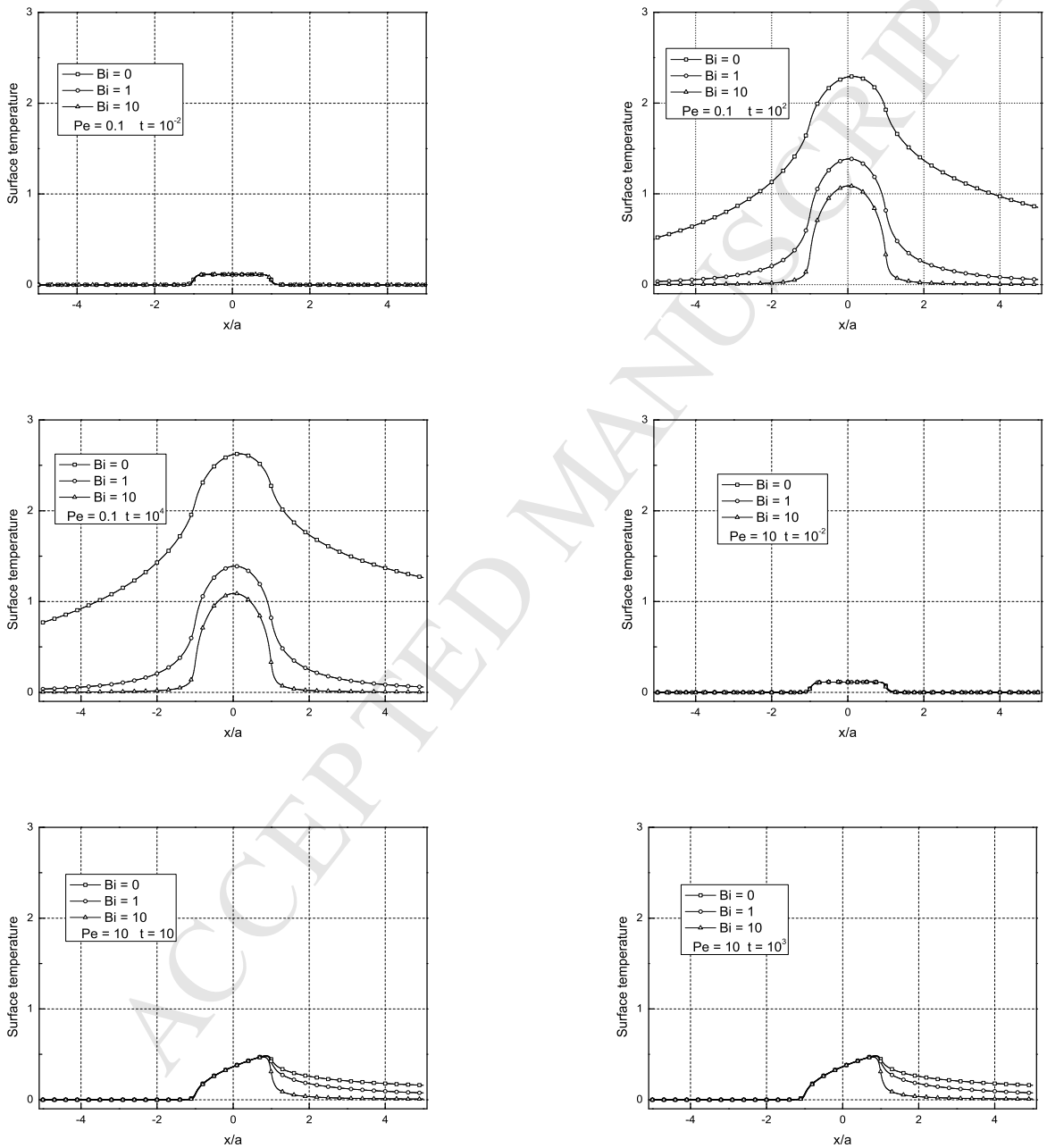


Figure 9: Surface temperature as a function of time for two Peclet numbers and three cooling cases (transient state).

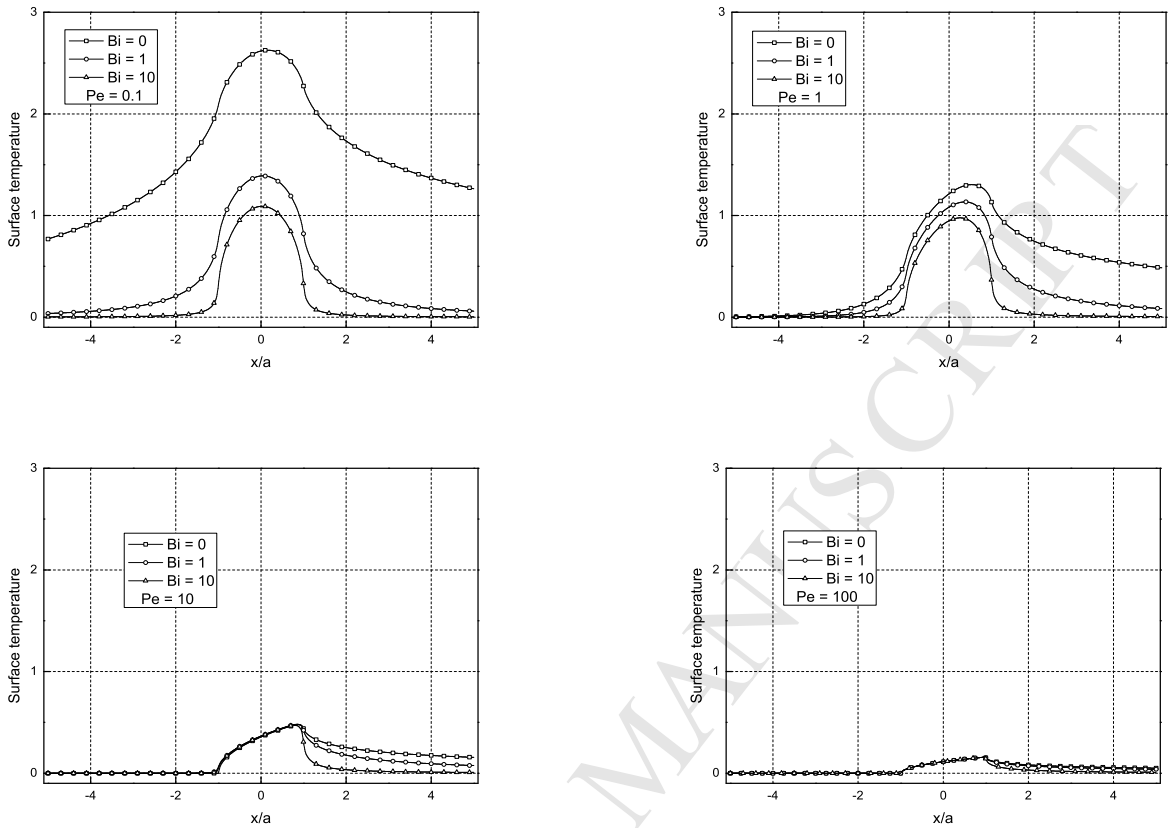


Figure 10: Stationary surface temperature for four Peclet numbers and three cooling cases (steady state).

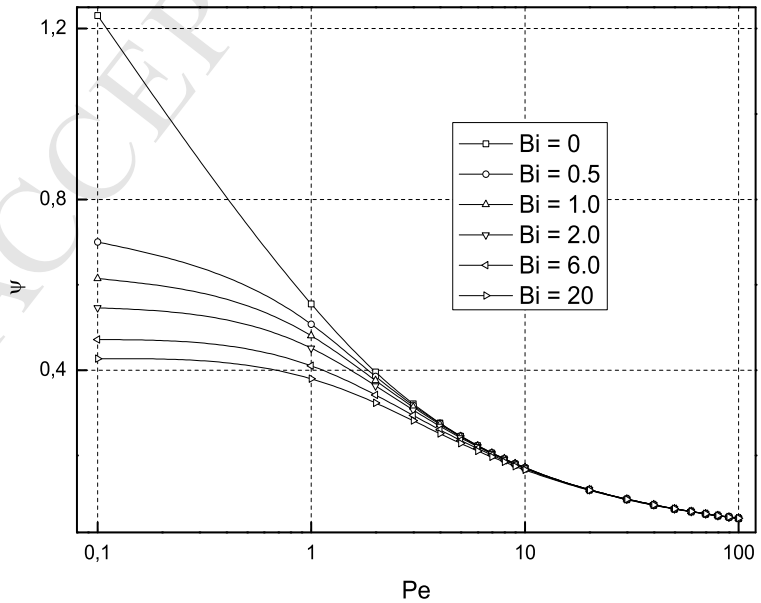


Figure 11: Constriction resistance as a function of Peclet for different Biot numbers.

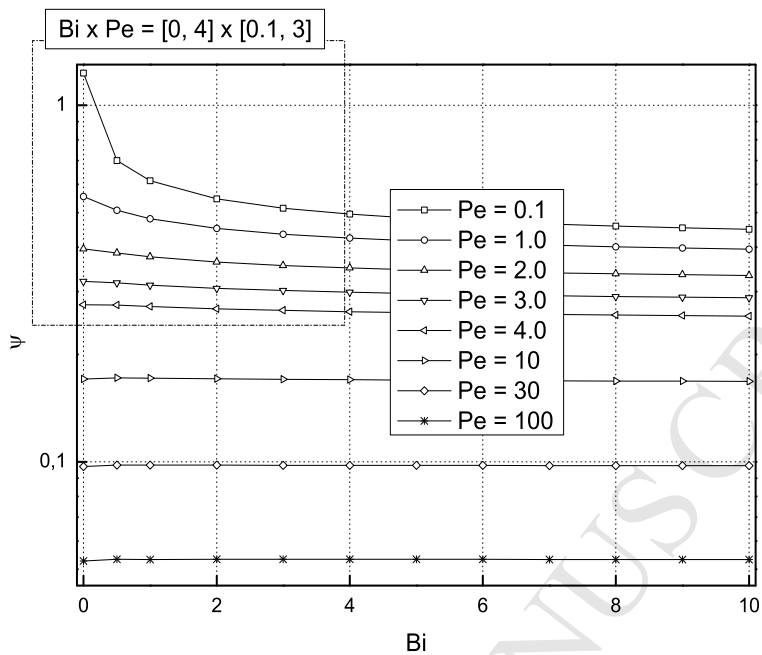


Figure 12: Constriction resistance as a function of Biot for different Peclet numbers.

outside the previously mentioned window. At a high Peclet number, the presented curves run parallel as a function of $Bi$ and clearly show no effect of cooling on the constriction resistance. The constriction parameter is a function of two variables $Bi$ and $Pe$, i.e. $\psi(Bi, Pe)$, and a three dimensional graphic representation is better in this case.

| Case | Eq. | $Bi$ | $A$ | $B$ | $C$ | R-square |
|---|---|---|---|---|---|---|
| | | 0 | 0.547 | -0.468 | -0.012 | 0.998 |
| $\psi_{ss} = APe^B + C$ | (29) | 1 | 0.508 | -0.359 | -0.047 | 0.992 |
| | | 10 | 0.486 | -0.257 | -0.099 | 0.988 |
| $\psi_{ss} = AB^{Bi}Pe^C$ | (30) | | 0.418 | 0.964 | -0.237 | 0.888 |

Table 2: Least square fitting of $\psi_{ss}$ as a function of $Bi$ and $Pe$. Equation (29) gives the steady state value of $\psi$ for different values of $Bi$. Equation (30) gives the steady state $\psi$ as a function of $Bi$ and $Pe$ at the same time.

A nonlinear least square fitting is conducted to derive analytical formulae, which are ready for use in approximating the steady state constriction resistance as a function of both $Bi$ and $Pe$ with and without cooling. Table (2) summarizes the obtained fitted parameters for two different cases :

- The first and simplest interpolation concerns the approximation of $\psi_{ss}$ as a function of $Pe$ without incorporating the cooling effect and this is accomplished through equation (29). For each value of $Bi$ a set of parameter ($A$, $B$ and $C$) is deduced from the fitting. As shown by the R-square value $R$, the approximation in this case is excellent.

- The second fitting model is expressed by equation (30). This is the most difficult case to conduct due to the strong nonlinearity of steady state constriction resistance $\psi_{ss}$ as a function of $Bi$ and $Pe$ simultaneously. The fitting quality is acceptable but need an extra work to be improved.

The constriction rise at the origin is obtained for different values of $Bi$ and shown in Figure (12) as a function of the Peclet number. The constriction at the origin is found to be substantially reduced with the increasing of $Bi$ when the Peclet number is less than three.

## Conclusions

A general analytical solution for the temperature rise at any point due to a stationary or moving band heat source with uniform heat intensity distribution was developed based on Jaeger's classical heat source method. This solution can be used for both transient and steady state conditions without convection outside the contact area. It can also be used to determine the surface temperature distribution and dimensionless constriction resistance in the half-space. For a moving heat source, the location of the point of maximum steady state temperature rise is shown to be different for different Peclet numbers.

A numerical solution has been developed to study the influence of cooling on the evolution of surface temperature and the constriction resistance. This solution was first validated by the analytical solution for adiabatic boundary conditions where an error of 0.10 % was observed. The numerical results obtained from the developed model highlighted the inter-related roles of three parameters considered in the present work: the velocity, the heat convection coefficient, and the thermal constriction resistance. This study shows an appreciable effect of cooling on the temperature field in the half space at a low Peclet number resulting in weak constriction resistance. This effect is minimized by the increase of the heat strip source speed.

The analysis of the obtained results shows that the increase of the velocity reduces the penetration of the thermal heat in the half space. The cooling increase significantly reduces the temperature gradient, in particular in the vicinity of the frictional surface. Finally, some correlations are given to evaluate the time interval for which the steady state is reached, and to estimate the constriction parameter as a function of Peclet and Biot numbers in the steady state case. The establishment of constriction resistance is affected by the heat source velocity. The establishment time is short when the speed is high and vice-versa.

## References


[1] Carslaw H.S. and Jaeger J.C. *Conduction of Heat in Solids.* Oxford University Press, London, 1959.

[2] Jaeger J.C. Moving sources of heat and the temperature at sliding contacts. *Proc. Roy. Soc. NSW*, 76:203–224, 1942.

[3] Archard J.F. The temperature of rubbing surfaces. *Wear*, 2:438–455, 1959.

[4] Bardon J.P. Physical bases of the imperfect thermal contact conditions between two bodies in relative motion. *Revue Générale de Thermique*, 386:86–91, 1994.

[5] Laraqi N. Températures de contact et coefficient de partage de flux généré par frottement sec entre deux solides. Approche nouvelle de la génération de flux. (*Contact temperature and flux partition coefficient of heat generated by dry friction between two solids. New approach to flux generation*). *International Journal of Heat and Mass Transfer*, 35(11):3131–3139, 1992.

[6] Laraqi N., Bairi A. and Ségui L. Tempertaure and thermal resistance in frictional devices. *Applied Thermal Engineering*, 24:2567–2581, 2004.

[7] Kounas P.S., Dimarogonas A.D. and Sandor G.N. The distribution of friction heat between a stationary pin and rotating cylinder. *Wear*, 19:415–424, 1972.

[8] Laraqi N. Velocity and relative contact size effect of the thermal constriction resistance in sliding solids. *ASME, Journal of Heat Transfer*, 119:173–177, 1997.

[9] Laraqi N. Phénomène de constriction thermique dans les contacts glissants. (*Thermal constriction phenomenon in sliding contacts*). *International Journal of Heat and Mass Transfer*, 39(17):3717–3724, 1996.

[10] Laraqi N. Thermal impedance and transient temperature due to a spot of heat on a half space. *International Journal of Thermal Sciences*, 49:529–533, 2010.

[11] Cameron A., Gordon A.N. and Symm G.T. Contact temperature in rolling sliding surfaces. *Proc. Royal Soc. of London. Series A, Math. Physical Sciences*, 286:45–61, 1964.

[12] Hou Z.B. and Komanduri R. General solutions for stationary/moving plane heat source problems in manufacturing and tribology. *International Journal of Heat and Mass Transfer*, 43:1679–1698, 2000.

[13] Yevtushenko A. and Kuciej M. Temperature and thermal stresses in the pad/disc during braking. *Applied Thermal Engineering*, 30:354–359, 2010.

[14] Grzes P. and Adamowicz A. Analysis of disc brake temperature distribution during single braking under non-axisymmetric load. *Applied Thermal Engineering*, doi:10.1016/j.applthermaleng.2010.12.016, 2011.

[15] Salti B. and Laraqi N. 3-D numerical modelling of heat transfer between two sliding bodies: temperature and thermal contact resistance. *International Journal of Heat and Mass Transfer*, 42:2363–2374, 1999.

[16] Jing L. and Li J.C.M. Temperature distribution in workpiece during scratching and grinding. *Materials Science and Engineering A*, 409:108–119, 2005.

[17] Tian X. and Kennedy F.E. Temperature rise at the sliding contact interface for a coated semi-infinite body. *ASME, Journal of Tribology*, 115:1–9, 1993.

[18] Rostami A.A., Hassan A., and Lim P.C. Parametric study of thermal constriction resistance. *Heat and Mass Transfer*, 37:5–10, 2001.

[19] Hamraoui M. Thermal behaviour of rollers during the rolling process. *Applied Thermal Engineering*, 29:2386–2390, 2009.

[20] Shuangbiao L., Lannou S., Qian W. and Leon K. Solutions for temperature rise in staionary/moving bodies caused by surface heating with surface convection. *ASME, Journal of Heat Transfer*, 126:779–785, 2004.

[21] Des Ruisseaux N.R. and Zerkle R.D. Temperature in semi-infinite and cylindrical bodies subjected to moving heat sources and surface cooling. *ASME J. Heat Transfer*, 08:456–464, 1970.

[22] Gecim B. and Winer W.O. Transient temperatures in the vicinity of an asperity contact. *ASME, Journal of Tribology*, 107:333–342, 1985.

[23] Talaat O. and Boucheffa A. Analytical solution for the 3-D steady state conduction in a solid subjected to a moving rectangular heat source and surface cooling. *Comptes Rendus Mecanique*, 337:107–111, 2009.

[24] Garcia J.M. and Laraqi N. Steady state temperature of two layer bodies subjected to a moving heat source and convected cooling. *International Journal of Thermal Sciences*, 49:756–761, 2010.

[25] Bairi A., Alilat N., Bauzin J.G. and Laraqi N. Three-dimensional stationnary thermal behavior of bearing ball. *International Journal of Thermal Sciences*, 43:561–568, 2004.

[26] Laraqi N., Alilat N., Garcia J.M. and Bairi A. Temperature and division of heat in a pin-on-disc frictional device - Exact analytical solution. *Wear*, 266:765–770, 2009.

[27] Turyk P.J. and Yovanovich M.M. Transient constriction resistance for elemental flux channels heated by uniform flux sources. *22nd Heat Transfer Conference*, ASME Paper No 84-HT-52, August, Niagara Falls, N.Y. 1984.

[28] Muzychka Y.S. and Yovanovich M.M. Thermal resistance models for non-circular moving heat sources on a half space. *ASME, Journal of Heat Transfer*, 123:624–632, 2001.

[29] Negus K.J., Yovanovich M.M. and Beck J.V. On the Nondimensionalization of Constriction Resistance for Semi-infinite Heat Flux Tubes. *ASME, Journal of Heat Transfer*, 111:804–807, August 1989.

[30] Madhusudana C.V. *Thermal contact conductance*. Springer-Verlag, New York, 1995.

[31] Yovanovich M.M. and Marotta E.E. *Heat Transfer Handbook, Bejan A., Krauss A.D. eds*, Chap: Thermal spreading and contact resistances, pages 261–393. John Wiley & Sons, New Jersey, 2003.

[32] Yovanovich M.M. *Handbook of Heat Transfer, Rohsenow W.M., Hartnett J.P. and Cho Y.L. eds*, Chap: Conduction and thermal contact resistance, pages 3.1–3.73. John Wiley & Sons, New York, 1998.

[33] Yovanovich M.M., Muzychka Y.S. and Culham J.R. Spreading resistance of isoflux rectangles and strips on compound flux channels. *Journal of Thermophysics and Heat Transfer*, 13(4):495–500, 1999.

[34] A.B. Comsol Multiphysics. Reference manuel. *Version 3.3*, 2003.

[35] Ling F.F., Lai W.M., Lucca D.A. *Fundamentals of Surface Mechanics with Applications*. Springer-Verlag, New York, 2002.

[36] Press W.H., Teukolsky S.A., Vetterling W.T., Flannery B.P. *Numerical Recipes in Fortran*. University Press, Cambridge, 1992.